

Research

Binding interaction studies of sodium benzoate, calcium propionate and sodium propionate with bovine serum albumin using spectroscopic method and molecular docking

Olayemi M. Adegbolagun¹ · Sarah C. Avong¹ · Oluwatobi O. Olakojo² · Yemi A. Adekunle³

Received: 28 March 2024 / Accepted: 17 October 2024

Published online: 28 October 2024

© The Author(s) 2024 **OPEN**

Abstract

The study investigated the in vitro interaction of bovine serum albumin (BSA) with sodium benzoate (SB), calcium propionate (CP) and sodium propionate (SP) and their consequent health impact on foods and pharmaceuticals when utilized as additives. The binding interaction studies of the compounds were investigated under simulated physiological conditions using spectroscopic analysis and molecular docking with thermodynamic parameters obtained to determine the nature of binding forces. The UV spectra for the three analytes revealed significant hypochromic effect of BSA-ligand interactions compared to only BSA indicating a modification of the BSA conformation due to possible hydrophobic interactions between the aromatic rings of the amino acids and ligands and other non-covalent interactions. Thermodynamic parameters obtained shows the binding interactions are exothermic, spontaneous, and hydrogen bonding and van der Waal's forces are chiefly responsible for formation and stabilization of BSA binding with SB, CP and SP and with additional pi-alkyl interactions observed for SB binding. Docking studies depict that hydrogen bonding was observed between the carbonyl group of SB and ARG256 residue of BSA and van der Waal forces also observed between SB and nine residues within the binding pocket of BSA. CP showed multiple hydrogen bonds between its carbonyl group and GLY247, LEU249 and LEU250 residues of BSA and SP also interacted with ARG256 of the protein via hydrogen bonding, and other amino acids via distance-dependent van der Waals forces. The study explains the binding mechanisms of the analytes with BSA and could determine their resultant pharmacodynamic effect on protein function when employed as food or pharmaceutical additives.

Keywords BSA binding studies · Hydrogen bonding · Molecular docking · Protein–ligand binding · Additives

1 Introduction

The use of additives has become a common practice in the food and pharmaceutical industries, this can be in form of colorants, flavors, antioxidants, and preservatives which have been known to improve the aesthetics, organoleptic properties and consequently the quality and shelf-life of the products [1, 2]. Sodium benzoate (SB), calcium propionate (CP) and sodium propionate (SP) are widely used as preservatives in foods and pharmaceuticals because of their anti-microbial activities.

✉ Oluwatobi O. Olakojo, oluwatobi.olakojo@fuoye.edu.ng; Olayemi M. Adegbolagun, duplag03@yahoo.com; Sarah C. Avong, avongsarah9@gmail.com; Yemi A. Adekunle, adekunleya@abuad.edu.ng | ¹Department of Pharmaceutical Chemistry, Faculty of Pharmacy, University of Ibadan, Ibadan, Nigeria. ²Department of Pharmaceutical and Medicinal Chemistry, Faculty of Pharmacy, Federal University Oye-Ekiti, Ekiti, Nigeria. ³Department of Pharmaceutical and Medicinal Chemistry, College of Pharmacy, Afe Babalola University Ado-Ekiti, Ekiti, Nigeria.



SB because of its ability to effectively inhibit fungal and bacterial growth during storage [3, 4] has found usefulness in a range of dishes and drinks, including salads, sodas, juices, jams, and soy sauce. It is also applicable clinically in the management of numerous illnesses, including Parkinson's disease, early Alzheimer's disease, multiple sclerosis, liver disease, and urea cycle abnormalities [5, 6]. CP is a microbial inhibitor in food, tobacco and pharmaceuticals. It is used in butyl rubber to improve process ability and scotching resistance. It has been applied to prolong the shelf life of several products like bread, other baked goods, processed meat, whey and dairy products [7]. SP has similar antimicrobial activity as calcium propionate where it inhibits mold growth in food and beverages. It is a component of baked foods, nonalcoholic drinks, cheeses, puddings and fillings, gelatins, jams and jellies, meat items and soft candies [8]. Despite that these preservatives are generally recognized as safe (GRAS), with concentration limits specified by the US Food and Drug Administration (FDA) [9], these substances are mostly products of chemical syntheses which pose threat to humans and their long-term usage can have potential risk to humans and alter the configuration of DNA and transport proteins such as serum albumin in human bodies. Understanding how these additives interact with serum albumin will help reveal their impact on health. Serum albumin, the most prevalent translocator protein in blood circulation [10, 11], performs a number of vital physiological tasks, including transporting various endogenous and exogenous compounds and maintaining colloidal osmotic blood pressure [12]. In addition to being widely used in pharmaceutical and biomedical applications, bovine serum albumin (BSA) is also frequently used as a ligand-biological model to research the interactions between small molecules and globular proteins. This is because of its excellent stability, affordability, adaptability, and relevance in medicine, as well as its strong structural similarity (about 76%) with human serum albumin [13]. About 583 amino acid residues make up the single-chain, globular protein BSA, which forms 17 disulfide linkages [14]. The hydrophobic cavities found in sub-domains II-A and III-A are also known as Sudlow's sites I and II, in that order, are host specialized ligand-binding sites in BSA [15]. As a result of the contact effect, prior research has shown that chemical toxicity and durability have a significant impact on the structure of BSA [16]. Additionally, numerous investigations have demonstrated that BSA's secondary structure changes when it binds to small molecules [17–19]. Therefore, it is crucial to research how BSA interacts with compounds, especially small molecules, hence this article is aimed at investigating the interaction between BSA and additives such as sodium benzoate, calcium propionate and sodium propionate. This will provide theoretical knowledge for the physiological properties of these additives and to promote the development of safe food and pharmaceutical additives. The study involves the use of UV spectroscopy and molecular docking to ascertain BSA's structure and conformation when it binds to the additives.

2 Experimental

2.1 Materials

Potassium dihydrogen phosphate, sodium hydroxide, sodium benzoate, calcium propionate and sodium propionate were all obtained from AK Scientific California, BSA from Glentham, UK.

2.2 Equipment

UV/Visible spectrophotometer (double beam PC 8 scanning autocell, UVD-3200, Labomed Inc.), pH meter (Mettler Toledo, PHS-3C).

2.3 Sample preparation

Phosphate buffer solution (PBS) of pH 7.4 was prepared by using potassium dihydrogen phosphate and sodium hydroxide according to the British Pharmacopoeia [20]. A 1×10^{-6} M stock solution of BSA was prepared by adding 0.0332 g of the sample to a 500 ml volumetric flask containing 200 ml PBS. It was gently mixed to dissolve and made up to volume with PBS. Stock solutions of each of sodium benzoate, calcium propionate and sodium propionate were prepared in aqueous medium to achieve a concentration of 1 mM and the eventual working concentrations in each case were 1, 2, 4, 6 and 8 μ M.

2.4 UV–Vis spectra analysis

Equal volumes of BSA and aliquot solution of the different concentrations of SB were placed in sample tubes to make a volume of 5 ml and the mixture was allowed to react together for a period of 10 min at a temperature of 25 °C. Similar procedures were carried out for CP and SP. The UV–visible spectra of BSA alone and with the samples were recorded from 200 to 400 nm while employing the corresponding ligand solution for baseline correction of the spectrophotometer. The entire procedure was carried out in triplicate and the experiment also repeated at 37 and 45 °C.

2.5 Molecular docking

The crystal structure of Bovine Serum Albumin (BSA) in complex with 3,5-diiodosalicylic acid was retrieved on <https://www.rcsb.org/> (Protein data bank, PDB ID: 4JK4). The protein has a resolution of 2.65 Å [21]. The 3D structures of SB, CP, and SP were retrieved from PubChem (<https://pubchem.ncbi.nlm.nih.gov/>). Both protein and ligands were prepared on UCSF Chimera 1.16, eliminating water molecules, co-crystallized ligand, and other molecules from the protein [22]. Structures minimisation and optimisation for protein was done at 200 steepest descent steps (and 100 steepest descent steps for ligands), 0.02 steepest descent steps size (Å), ten conjugate gradient steps, and 0.02 conjugate gradient steps size (Å) 10 update intervals using the structure editing wizard. Charges were then added to the ligands through ANTE-CHAMBER. The Autodock Vina of PyRx was used to speculate the binding interactions of SB, CP, and SP on BSA [23]. The binding site of the co-crystallized ligand on the protein was pre-defined using Chimera (at < 5 Å) and fifty-five (55) amino acid residues were implicated [24]. A site-directed docking was therefore carried out using the grid dimensions: Center X:87.6383 Y:23.5980 Z:26.1382; Dimensions (Angstrom) X:44.2478 Y:33.1153 Z:43.1179. Discovery Studio 2021 Client was used for molecular visualization.

3 Results and discussion

3.1 UV Spectrophotometric analysis

UV–vis spectroscopic technique can be used to explore the structural changes of protein and also look into the conformational changes that occur in proteins during their binding interactions with small molecular substances. The binding kinetics studies were carried out at three-level temperature; 25, 37 and 45 °C depicting room temperature, body temperature and the temperature obtained as a result of processing and milling during industrial activities respectively. Figures 1, 2, 3 showed the overlaid UV absorption spectra of the interaction of BSA with SB, CP and SP respectively at varying temperatures.

The UV spectra of BSA revealed two characteristic bands; one intense large band at 217 nm with an intensity of 0.447 and one weak band at 277 nm with an intensity of 0.047. The former is associated with the π – π^* transition of C=O functional groups in the peptide and carboxylic acid moieties in the compounds (N-terminal peptides as N–CHR–COOH and C–terminal peptide as NH₂–CHR–CO) and the latter with the π – π^* transition of the aromatic ring portions of hydrophobic amino acids (tryptophan, tyrosine, phenylalanine) in the BSA structure [25].

At 25 °C, the strong absorption band of BSA-SB was observed around 215 nm showing a slight hypsochromic shift ($\Delta\lambda = -2$ nm) which is due to the absorbance of peptides and carboxylic moieties into the protein compound. The addition of SB (from 1 to 8 μ M) to the BSA solution reduces the intensity from 0.279 to 0.2460 indicating a hypochromic effect. The weak absorption bands at 277 nm reveal a constant band across the aliquot concentrations with a decrease in the intensity from 0.026 to 0.018 indicating a hypochromic effect. A similar observation was recorded at 37 °C where a strong band was observed at 215 nm and the weak band at 276 nm indicating a slight hypsochromic shift of 1 nm. However, at 45 °C, the high intensity band BSA-SB shifted 3 nm short of the free BSA with reduce absorbance upon titration with increased concentration of SB. The weak absorption band were observed at 277 nm with an hypsochromic effect observed just like at previous temperatures recorded. When BSA was titrated with CP, UV spectra also showed similar patterns across the temperature levels considered with strong intensity band appearing between 214 and 217 nm and the weaker band at 277 nm, however with reduced absorbance value as the concentration of ligand increases. The same pattern was observed with SP save that the low intensity bands were observed at 278 nm ($\Delta\lambda = +1$ nm).

Fig. 1 Overlaid UV absorption spectra of BSA alone and BSA with varying concentrations of SB at 25 (a), 37 (b) and 45 °C (c)

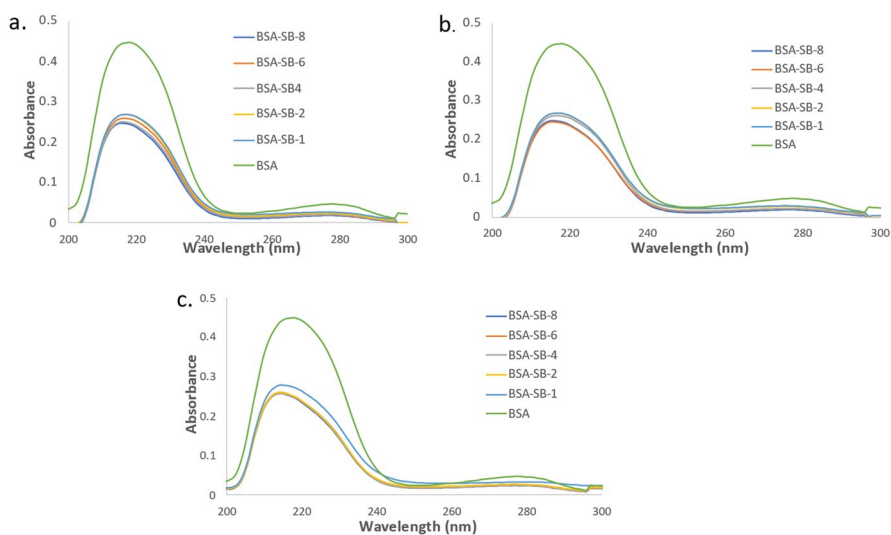


Fig. 2 Overlaid UV absorption spectra of BSA alone and BSA with varying concentrations of CP at 25 (a), 37 (b) and 45 °C (c)

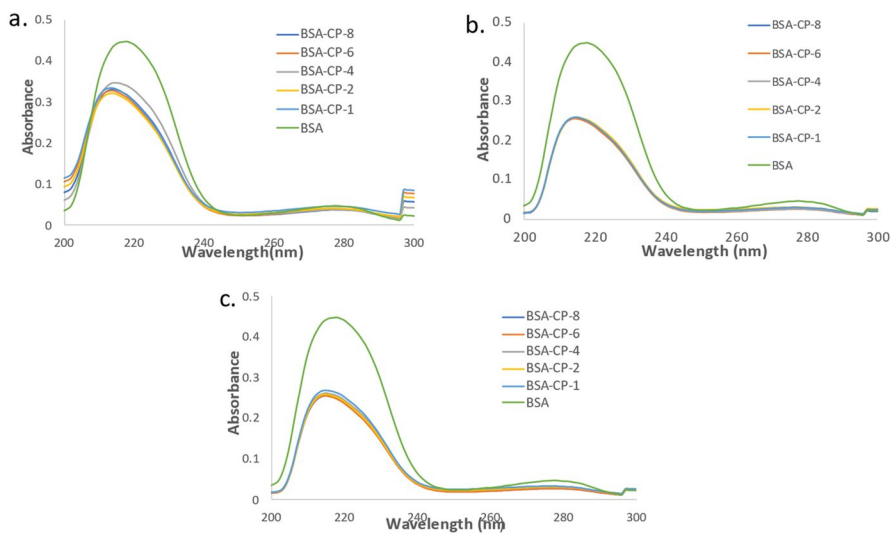
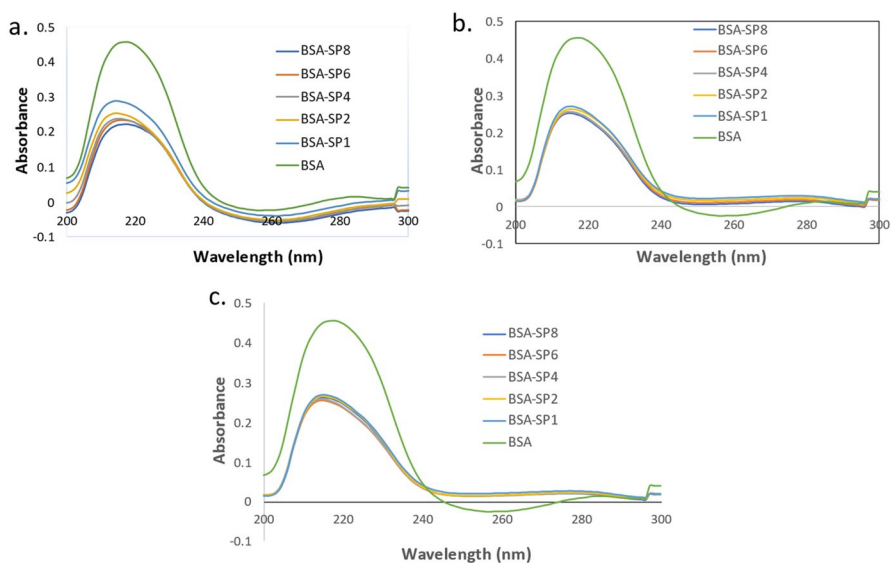


Fig. 3 Overlaid UV absorption spectra of BSA alone and BSA with varying concentrations of SP at 25 (a), 37 (b) and 45 °C (c)



In all, it can be seen that a marked hypochromic effect was observed with BSA-ligand interactions relative to the neat BSA in the higher energy band. The changes observed in the absorbance could be due to hydrophobic interactions between the aromatic rings of the amino acids and the ligands. These changes signify a modification in the BSA conformation which could result in the backbone unfolding and increase the hydrophobicity of the microenvironment of the aromatic amino acid residues [26]. It could also be due to hydrogen bonding, electrostatic forces or van der Waal's interactions.

3.2 Binding studies

Essentially, there are two types of binding involved in ligand-biomolecular interactions: the reversible non-covalent and the irreversible or covalent binding. In non-covalent interactions, the collaborating atoms do not share electrons and are weaker than covalent connections. They are of great importance in biochemical processes, where they determine the structure, dynamics, and function of biomolecules [27, 28]. They are, nevertheless, distinct, appealing and being reversible, can be built and broken without consuming much energy. They also have an impact on pharmacokinetic properties of molecules such as solubility, partitioning, distribution, and permeability, which are critical to medication development and functionality [29]. Their interactions could be within the amino acids of the protein or inter-molecularly between the protein and the ligand in a protein–ligand complex [30]. Intermolecular forces, such as ionic bonds, hydrogen bonds and Van der Waals forces, are responsible for non-covalent ligand-binding interactions and these associations with ligands are almost always reversible. On the other hand, covalent bonds are created when a reactive functional group of the ligand, such as hydroxyl, epoxy, or carbonyl, interacts with a nucleophilic cysteine, serine, threonine, or, in rare cases, lysine. This process creates covalent adducts [31]. This bond forms an irreversible bond within the target protein's half-life and is long enough to produce a ligand–protein complex that is not susceptible to classical equilibrium [32]. It has been demonstrated that substances that are genotoxic can bind covalently to nuclear proteins (as against genotoxicity as a result of covalent bond formation with DNA) [33].

The binding constants of ligands SB, CP and SP were determined at the three temperature levels using nonlinear regression based on the quadratic equation [34] stated below:

$$\frac{A_0 - A}{A_0} = ([P] + [L] + K_f) - \frac{\sqrt{([P] + [L] + K_f)^2 - 4[P][L]}}{2[P]} \quad (1)$$

where A_0 and A are the absorbance of free and bound BSA respectively, $\frac{A_0 - A}{A_0}$ is the fraction of bound ligand, $[P]$ and $[L]$ are the concentrations of the protein and ligand respectively while K_f is the binding constant, these parameters are determined mathematically using nonlinear regression in the Eq. (1). The binding curve when fraction of bound ligand is plotted against its concentration the graphs are in Figs. 4, 5, 6, while the binding constants, K_f obtained are depicted in Table 1.

3.3 Thermodynamic parameters and nature of binding forces

The estimation of thermodynamic parameters is critical to gain further insight into how BSA binds to dietary ingredients. The overall free energy change (ΔG) was calculated using Eq. (2)

$$\Delta G = -RT \ln K \quad (2)$$

where T is the temperature in Kelvin and R is the universal gas constant. The modified Van't Hoff Eq. (3) and (4) was used to calculate the thermodynamic enthalpy (ΔH) and entropy (ΔS) change of BSA and ligand complexation. Enthalpy change is derived from the slope using Eq. (4) and entropy change from the intercept when the natural logarithm of the binding constants K_f is plotted against the reciprocal of the temperatures (T).

$$\Delta G = \Delta H - T\Delta S \quad (3)$$

$$\ln k = -\frac{\Delta H}{RT} + \frac{\Delta S}{R} \quad (4)$$

The thermodynamic parameters for the food additives were derived as shown in Table 1.

For the binding interactions of the ligands with BSA except for BSA-CP where a more stable complex was formed with temperature, the binding constants decreased slightly with increasing temperature which depicts that this is

Fig. 4 Non-linear regression plots for the formation of BSA-SB complex at 25, 37 and 45 °C

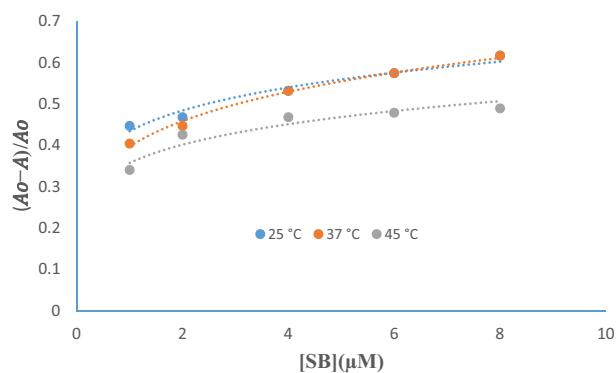


Fig. 5 Non-linear regression plots for the formation of BSA-CP complex at 25, 37 and 45 °C

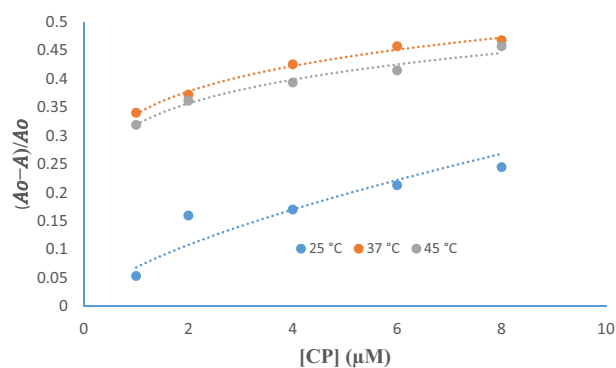


Fig. 6 Non-linear regression plots for the formation of BSA-SP complex at 25, 37 and 45 °C

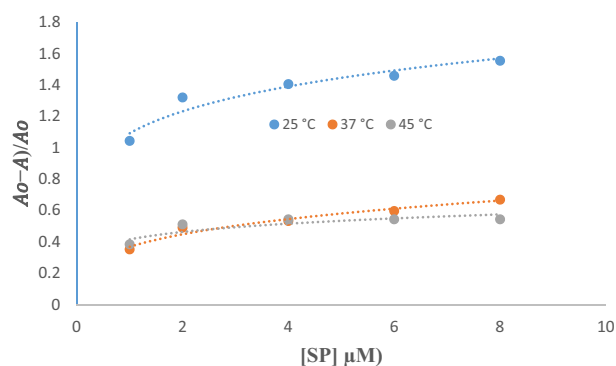


Table 1 Thermodynamic energy fluctuations and binding connected to BSA's interaction with ligands

| Binding | 25 °C | | 37 °C | | 45 °C | | ΔH (KJ mol ⁻¹) | ΔS (J K ⁻¹) |
|---------|-----------|------------------------------------|-----------|------------------------------------|-----------|------------------------------------|------------------------------------|---------------------------------|
| | $\ln K_f$ | ΔG (KJ mol ⁻¹) | $\ln K_f$ | ΔG (KJ mol ⁻¹) | $\ln K_f$ | ΔG (KJ mol ⁻¹) | | |
| BSA-SB | 12.72 | -31.52 | 12.72 | -32.79 | 12.70 | -33.59 | 0.64 | -103.66 |
| BSA-CP | 12.66 | -31.36 | 12.70 | -32.73 | 12.69 | -33.57 | -1.71 | -110.99 |
| BSA-SP | 12.91 | -31.98 | 12.72 | -32.80 | 12.72 | -33.63 | -7.88 | -80.74 |

an exothermic reaction process. The negative free energy changes obtained with regards to the formation of the complexes for all the binding interactions reveal that the binding is spontaneous. The consideration of enthalpy and entropy change to the free energy change plays a contributory role in the determination of major type of interaction responsible for binding of the ligand to the biomolecule. Based on previous research [35, 36], it was reported that if the value of ΔH and ΔS are negative, van der Waal's interactions and hydrogen bonds are mainly responsible for the binding reaction. If the value of ΔH and ΔS are positive, hydrophobic interactions are most prominent while

electrostatic forces are more important when ΔH value is negative and ΔS value is positive. The minute positive value of ΔH and the negative ΔS value associated with the interaction of BSA with SB indicate that hydrogen bonding and hydrophobic interactions are probable in the formation and stabilization of the ligand–protein complex. This is not unlikely as sodium benzoate when in solution dissociate to form ions and charge distribution can occur between the ions and the ionic sites of the side chain of amino acids that are constituents of the BSA. The resultant effect of this could impact pharmacokinetic and pharmacodynamic activities when SB is employed as a pharmaceutical excipient or as food additives. Hydrophobic interaction between the aromatic residue of SB can also occur with the hydrophobic pockets of BSA and this is also depicted in the molecular docking studies (Fig. 7). However, the negative values of ΔH and ΔS obtained with BSA-CP and BSA-SP suggest that the protein-complex formation is driven by, van der Waal's interactions and hydrogen bonding. Thus, the binding stabilizing the complex formation is likely between carboxylic functional group of the structure of the propionates and the amino functions of the albumin. Yu and coworkers [37] have also investigated the binding interaction of BSA with SB using spectroscopic and molecular docking studies but this research as far as we are aware is the first investigation of BSA interaction with CP and SP.

3.4 Molecular docking

Molecular docking studies were conducted to gain insights into the positions of favourable interactions between the ligands and BSA [38]. The 3-dimensional structure of BSA retrieved from PDB had 3,5-diiodosalicylic acid as co-crystallised ligand. CP, SB, and SP were docked to the binding pocket of 3,5-diiodosalicylic acid, and eight (8) exhaustive poses were obtained for each ligand. From the results in Table 2, the most affinity for BSA was exhibited by SB, whose binding energies were -5.9 kcal/mol. (RMSD = 0 Å). This is followed by SP with binding affinity of -4.1 kcal/mol, and CP having binding energy of -3.7 kcal/mol.

The binding energies (in kcal/mol) obtained for the ligands are justified by the types and numbers of intermolecular interactions involved. SB was noted to utilise H-bonding, π -alkyl interaction, and van der Waals forces to bind to BSA (Fig. 7). A hydrogen bonding was observed between the carbonyl functional group of SB and the guanidinium ion of ARG 256 residue of BSA. van der Waal's forces were also observed between SB and nine residues within the binding pocket of BSA (TYR149, ARG217, LEU218, LYS221, HIS241, LEU259, ALA260, ILE263, and ILE289). H-bonding and van der Waals interactions are important non-covalent bonds for proteins' molecular recognition by ligands [39]. In addition, the benzene unit formed π -alkyl interactions with the isobutyl group of LEU 237 and methyl group of ALA 290. These interactions corroborate the results obtained from the in vitro studies. CP showed multiple hydrogen bonds between carbonyl functional group and GLY247, LEU249 and LEU250 residues (Fig. 8) and van der Waals interactions with ALA26, VAL23, PHE70, LEU46, LEU66, ASP248 and HIS67 while SP which had the second highest binding affinity, was posed in such a way that it interacted with ARG256 via H bonding and with TYR149, LEU237, HIS241, LEU259, ALA260, ILE263, SER286, ILE289 and ALA290 via the distance-dependent van der Waals forces (Fig. 9). H-bonds contribute about 10–40 kJ/mol energy to protein–ligand binding [40].

Fig. 7 Visualisation of SB structure interacting with BSA in 3D (A) and 2D (B) showing H-bond, π -alkyl interaction, and van der Waals interaction

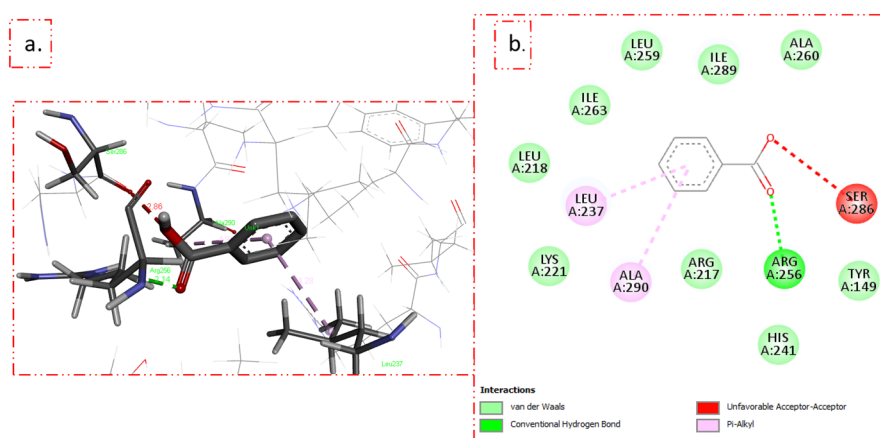


Table 2 Binding affinity scores of the three additives (ligands) when docked on BSA

| Rank | Binding affinity (kcal/mol) | | |
|------|-----------------------------|------|------|
| | SB | CP | SP |
| 1 | -5.9 | -3.7 | -4.1 |
| 2 | -5.5 | -3.6 | -3.7 |
| 3 | -5.5 | -3.6 | -3.6 |
| 4 | -5.5 | -3.6 | -3.6 |
| 5 | -5.4 | -3.4 | -3.6 |
| 6 | -5.4 | -3.3 | -3.4 |
| 7 | -5.4 | -3.2 | -3.3 |
| 8 | -5.3 | -3.2 | -3.3 |

4 Conclusion

The binding interactions of SB, CP, and SP with BSA were investigated using the UV-visible spectroscopic and molecular docking methods. Spectroscopic results showed a marked hypochromic effect with increased concentration of ligands relative to the BSA alone. Also, the binding constant increased with temperature revealing that a more stable ligand-protein complex is formed at higher temperature. The investigation of thermodynamic parameters showed that electrostatic force is prominent in the binding of SB to BSA and hydrophobic interactions as the major forces driving the interaction of BSA with both CP and SP. Molecular docking results revealed that H bonds, π -alkyl interaction, and van der Waals forces play roles in the binding of SB, CP, and SP to BSA. One important limitation of this study which is hereby acknowledged to ensure a comprehensive understanding of the study's findings is that only one spectroscopic study (UV spectroscopy) was employed. While molecular docking provided complementary information, a multi-spectroscopic studies could add to the robustness of the conclusions. Thus, the claim of this study can be verified upon its subject to other spectroscopic methods such as circular dichroism or fluorescence spectroscopy which are beyond the scope of this study.

Fig. 8 Visualisation of CP structure interacting with BSA in 3D (A) and 2D (B) showing H-bond and van der Waals interaction

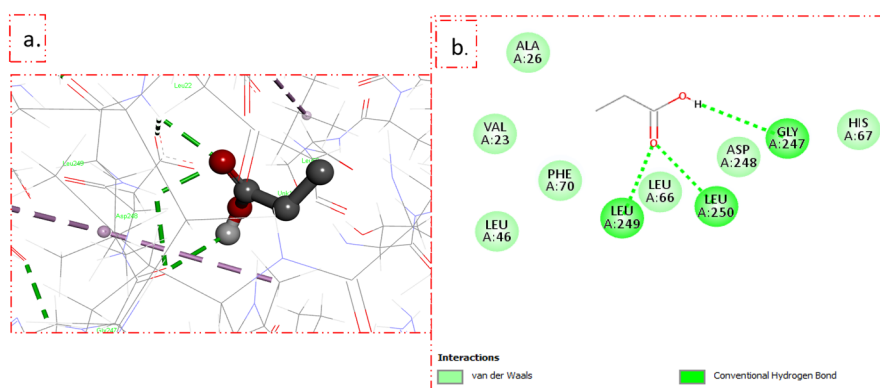
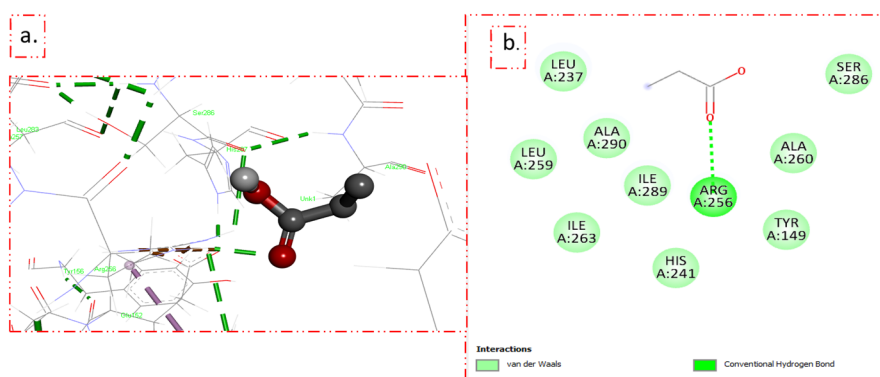


Fig. 9 Visualisation of SP structure interacting with BSA in 3D (A) and 2D (B) showing H-bond and van der Waals interaction



Acknowledgements We would like to appreciate the Technologists in the Department of Chemistry, University of Ibadan for their support during the laboratory procedures.

Author contributions OMA designed and supervised the study. Material preparation, data collection and analysis were performed by SCA and OOO. Further data interpretation was by YAA. The first draft of the manuscript was written by OOO and YAA and all authors commented on previous versions of the manuscript. Figures 1, 2, 3, 4, 5, 6 and Table 1 were prepared by OOO while Figs. 7, 8, 9 and Table 2 were prepared by YAA. All authors read and approved the final manuscript.

Funding The authors declare that no funds or grants was received for the purpose of this research.

Data availability Data supporting the findings of this submission can be accessed via this link: <https://shorturl.at/FD2mS>.

Declarations

Competing interests The authors declare no competing interests.

Open Access This article is licensed under a Creative Commons Attribution-NonCommercial-NoDerivatives 4.0 International License, which permits any non-commercial use, sharing, distribution and reproduction in any medium or format, as long as you give appropriate credit to the original author(s) and the source, provide a link to the Creative Commons licence, and indicate if you modified the licensed material. You do not have permission under this licence to share adapted material derived from this article or parts of it. The images or other third party material in this article are included in the article's Creative Commons licence, unless indicated otherwise in a credit line to the material. If material is not included in the article's Creative Commons licence and your intended use is not permitted by statutory regulation or exceeds the permitted use, you will need to obtain permission directly from the copyright holder. To view a copy of this licence, visit <http://creativecommons.org/licenses/by-nc-nd/4.0/>.

References

1. Kamal AA, Fawzia SA. Toxicological and safety assessment of tetrazine as a synthetic food additive on health biomarkers. *Afr J Biotech*. 2018;17:139–49. <https://doi.org/10.5897/AJB2017.16300>.
2. Indhiabor JE, Yakubu JM, Ezeonu SC. Effects of food additives and preservatives on man: a review. *Asian J Sci Technol*. 2015;6(2):1118–35.
3. Lennerz BS, Vafai SB, Delaney NF, Clish AB, Deik AA, Pierce KA, Ludwig DS, Mootha VK. Effect of sodium benzoate, a widely used food preservative, on glucose homeostasis and metabolic profiles in humans. *Mol Genet Metab*. 2015;114(1):73–9. <https://doi.org/10.1016/j.ymgme.2014.11.010>.
4. Nettis E, Colanardi MC, Ferrannini A. Sodium benzoate-induced repeated episodes of acute urticaria/angio-oedema: randomized controlled trial. *Br J Dermatol*. 2004;151(4):898–902. <https://doi.org/10.1111/j.1365-2133.2004.06095.x>.
5. Yavav A, Kumar A, Das M, Tripathi A. Sodium benzoate, a food preservative, affects the functional and activation status of splenocytes at non cytotoxic dose. *Food Chem Toxicol*. 2016;88:40–7. <https://doi.org/10.1016/j.fct.2015.12.016>.
6. Häberle J, Boddaert N, Burlina A, Chakrapani A, Dixon M, Huemer M, Karall D, Martinelli D, Crespo PS, Santer R, Servais A, Valayannopoulos V, Lindner M, Rubio V, Dionisi-Vici C. Suggested guidelines for the diagnosis and management of urea cycle disorders. *Orphanet J Rare Dis*. 2012;7(1):32. <https://doi.org/10.1186/1750-1172-7-32>.
7. Belz MCE, Mairinger R, Zannini E, Ryan LAM, Cashman KD, Arendt EK. The effect of sourdough and calcium propionate on the microbial shelf-life of salt reduced bread. *Appl Microbiol Biotechnol*. 2012;96(2):493–501. <https://doi.org/10.1007/s00253-012-4052-x>.
8. Kagliwal LD, Jadhav SB, Singhal RS, Kulkarni PR. Permitted preservatives. In: *Encyclopedia of food microbiology*. 2nd ed. Elsevier; 2014. pp. 99–101.
9. Misel ML, Gish RG, Patton H, Mendler M, Pahan K. Immunomodulation of experimental allergic encephalomyelitis by cinnamon metabolite sodium benzoate. *Immunopharmacol Immunotoxicol*. 2011;33(4):586–93. <https://doi.org/10.3109/08923973.2011.561861>.
10. Zhang Q, Ni Y, Kokot S. Competitive interactions between glucose and lactose with BSA: which sugar is better for children? *Analyst*. 2016;141(7):2218–27. <https://doi.org/10.1039/c5an02420j>.
11. Leblanc A, Shiao TC, Roy R, Sleno L. Absolute quantitation of NAPQI-modified rat serum albumin by LC-MS/MS: monitoring acetaminophen covalent binding in vivo. *Chem Res Toxicol*. 2014;27(9):1632–9. <https://doi.org/10.1021/tx500284g>.
12. Janek T, Czyżnikowska Ż, Łuczyński J. Physicochemical study of biomolecular interactions between lysosomotropic surfactants and bovine serum albumin. *Colloids Surf B*. 2017;159:750–8. <https://doi.org/10.1016/j.colsurfb.2017.08.046>.
13. Li D, Zhu J, Jin J, Yao X. Studies on the binding of nevadensin to human serum albumin by molecular spectroscopy and modeling. *J Mol Struct*. 2007;846:34–41. <https://doi.org/10.1016/j.molstruc.2007.01.020>.
14. Chaturvedi SK, Ahmad E, Khan JM, Alam P, Ishtikhar M, Khan RH. Elucidating the interaction of limonene with bovine serum albumin: a multi-technique approach. *Mol Bio Syst*. 2015;11(1):307–16. <https://doi.org/10.1039/c4mb00548a>.
15. Guan J, Yan X, Zhao YJ, Sun YH, Peng X. Binding studies of triclocarban with bovine serum albumin: insights from multi-spectroscopy and molecular modeling methods. *Spectrochim Acta A*. 2018;202:1–12. <https://doi.org/10.1016/j.saa.2018.04.070>.
16. Shi JH, Zhou KL, Lou YY, Pan DQ. Multi-spectroscopic and molecular modeling approaches to elucidate the binding interaction between bovine serum albumin and darunavir, a HIV protease inhibitor. *Spectrochim Acta A*. 2018;188:362–71. <https://doi.org/10.1016/j.saa.2017.07.040>.
17. Skrt M, Benedik E, Podlipnik C, Poklar UN. Interactions of different polyphenols with bovine serum albumin using fluorescence quenching and molecular docking. *Food Chem*. 2012;135(4):2418–24. <https://doi.org/10.1016/j.foodchem.2012.06.114>.

18. Tian J, Liu J, He W, Hu Z, Yao X, Chen X. Probing the binding of scutellarin to human serum albumin by circular dichroism, fluorescence spectroscopy, FTIR, and molecular modeling method. *Biomacromol.* 2004;5(5):1956–61. <https://doi.org/10.1021/bm049668m>.
19. Makarska-Bialokoz M. Investigation of the binding affinity in vitamin B12-Bovine serum albumin system using various spectroscopic methods. *Spectrochim Acta A.* 2017;184:262–9. <https://doi.org/10.1016/j.saa.2017.05.014>.
20. British Pharmacopoeia. Vol 5 Appendix 1D. London: The Stationery Office; 2020.
21. Sekula B, Zielinski K, Bujacz A. Crystallographic studies of the complexes of bovine and equine serum albumin with 3,5-diiodosalicylic acid. *Int J Biol Macromol.* 2013;60:316–24. <https://doi.org/10.1016/j.ijbiomac.2013.06.004>.
22. Pettersen EF, Goddard TD, Huang CC, Couch GS, Greenblatt DM, Meng EC, Ferrin TE. UCSF Chimera—a visualization system for exploratory research and analysis. *J Comput Chem.* 2004;25(13):1605–12. <https://doi.org/10.1002/jcc.20084>.
23. Trott O, Olson AJ. AutoDock Vina: improving the speed and accuracy of docking with a new scoring function, efficient optimization, and multithreading. *J Comput Chem.* 2010;31:455–61. <https://doi.org/10.1002/jcc.21334>.
24. Salentin S, Haupt VJ, Daminelli S, Schroeder M. Polypharmacology rescored: Protein-ligand interaction profiles for remote binding site similarity assessment. *Prog Biophys Mol Biol.* 2014;116(2–3):174–86. <https://doi.org/10.1016/j.pbiomolbio.2014.05.006>.
25. Dieaconu M, Ioanid A, Iftimie S, Antohe S. UV-Absorption mechanisms of Ni-binding bovine serum albumin. *Dig J Nanomater Biostruc.* 2012;7:1125–38.
26. Al Bratty M. Spectroscopic and molecular docking studies for characterizing binding mechanism and conformational changes of human serum albumin upon interaction with Telmisartan. *Saudi Pharm J.* 2020;28:729–36. <https://doi.org/10.1016/j.jsps.2020.04.015>.
27. Panigrahi SK, Desiraju GR. Strong and weak hydrogen bonds in the protein–ligand interface. *Prot Struct Funct Bioinform.* 2007;67:128–41. <https://doi.org/10.1002/prot.21253>.
28. Řezáč J, Hobza P. Benchmark calculations of interaction energies in noncovalent complexes and their applications. *Chem Rev.* 2016;116:5038–71. <https://doi.org/10.1021/acs.chemrev.5b00526>.
29. Desiraju GR. C–H···O and other weak hydrogen bonds. From crystal engineering to virtual screening. *Chem Commun.* 2005;24:2995–3001. <https://doi.org/10.1039/B504372G>.
30. Mahadevi AS. Cooperativity in noncovalent interactions. *Chem Rev.* 2016;116:2775–825. <https://doi.org/10.1021/cr500344e>.
31. Imane B, Olotu F, Agoni C, Adeniji E, Khan S, Rashedy A, Cherqaoui D, Soliman M. Covalent inhibition in drug discovery: filling the void in literature. *Curr Top Med Chem.* 2018;18:1–11. <https://doi.org/10.2174/1568026618666180731161438>.
32. James CP, Juliana LA, Özlem DE, Karen EJ. Irreversible inhibitors of serine, cysteine, and threonine proteases. *Chem Rev.* 2002;102:4639–750. <https://doi.org/10.1021/cr010182v>.
33. Enoch SJ, Ellison CM, Schultz TW, Cronin MTD. A review of the electrophilic reaction chemistry involved in covalent protein binding relevant to toxicity. *Crit Rev Toxicol.* 2011;41(9):783–802. <https://doi.org/10.3109/10408444.2011.598141>.
34. Jarmoskaite I, AlSadhan I, Vaidyanathan PP, Herschlag D. How to measure and evaluate binding affinities. *Biochem Chem Biol.* 2020;9:e57264. <https://doi.org/10.7554/eLife.57264>.
35. Khan SN, Islam B, Yennamalli R, Sultan A, Subbarao N, Khan AU. Interaction of mitoxantrone with human serum albumin: spectroscopic and molecular modeling studies. *Eur J Pharm Sci.* 2008;35:371–82. <https://doi.org/10.1016/j.ejps.2008.07.010>.
36. Chi Z, Liu R, Teng Y, Fang X, Gao C. Binding of oxytetracycline to bovine serum albumin: spectroscopic and molecular modeling investigations. *J Agric Food Chem.* 2010;58:10262–9. <https://doi.org/10.1021/jf101417w>.
37. Kuntz ID, Blaney JM, Oatley SJ, Langridge R, Ferrin TE. A geometric approach to macromolecule–ligand interactions. *J Mol Biol.* 1982;161:269–88. [https://doi.org/10.1016/0022-2836\(82\)90153-x](https://doi.org/10.1016/0022-2836(82)90153-x).
38. Yu J, Liu JY, Xiong WM, Zhang XY, Zheng Y. Binding interactions of sodium benzoate on BSA: multi spectroscopy and molecular docking studies. *BMC Chem.* 2019;13(1):95–102. <https://doi.org/10.1186/s13065-019-0615-6>.
39. Salentin S, Haupt VJ, Daminelli S, Schroeder M. Polypharmacology rescored: protein-ligand interaction profiles for remote binding site similarity assessment. *Prog Biophys Mol Biol.* 2014;116(2–3):174–86. <https://doi.org/10.1016/j.pbiomolbio.2014.05.006>.
40. Steiner T. The hydrogen bond in the solid state. *Angew Chem Int Ed.* 2002;41:49–76. <https://doi.org/10.1109/CDC.2015.7402694>.

Publisher's Note Springer Nature remains neutral with regard to jurisdictional claims in published maps and institutional affiliations.